

# The value of very low frequencies and far offsets for seismic data in the Permian Basin: Case study on a new dense survey from the Central Basin Platform

Vincent Durussel<sup>1</sup>, Dongren Bai<sup>2</sup>, Amin Baharvand Ahmadi<sup>2</sup>, Scott Downie<sup>1</sup>, and Keith Millis<sup>3</sup>

<https://doi.org/10.1190/tle41010034.1>

## Abstract

The depth of penetration and multidimensional characteristics of seismic waves make them an essential tool for subsurface exploration. However, their band-limited nature can make it difficult to integrate them with other types of ground measurements. Consequently, far offsets and very low-frequency components are key factors in maximizing the information jointly inverted from all recorded data. This explains why extending seismic bandwidth and available offsets has become a major industry focus. Although this requirement generally increases the complexity of acquisition and has an impact on its cost, improvements have been clearly and widely demonstrated on marine data. Onshore seismic data have generally followed the same trend but face different challenges, making it more difficult to maximize the benefits, especially for full-waveform inversion (FWI). This paper describes a new dense survey acquired in 2020 in the Permian Basin and aims to objectively assess the quality and benefits brought by a richer low end of the spectrum and far offsets. For this purpose, we considered several aspects, from acquisition design and field data to FWI imaging and quantitative interpretation.

## Introduction

Over the past decade, seismic data acquisition has seen greater emphasis in the recording and processing of far offsets as well as very low frequencies. By “very low frequencies,” we are essentially referring to the first octave of energy emitted by the source. In contrast, ultra-low frequencies, which can sometimes be present on seismic records due to natural and ambient noise, are not emitted by the active source (Le Meur et al., 2020). The benefits of very low frequencies on marine data have been shown by numerous authors for several crucial aspects of subsurface imaging, including velocity model building, reflector continuity, resolution, and quantitative interpretation (e.g., Duval, 2012; Sablon et al., 2012; ten Kroode et al., 2013; Reiser and Bird, 2016). For example, offshore surveys are increasingly being acquired with ocean-bottom nodes due to their strength in recording high-quality very low frequencies and long offsets for full-waveform inversion (FWI) (Yao et al., 2019). However, land seismic faces additional complications such as near-surface complexity, the presence of surface waves (which severely pollute the low end of the spectrum), and stronger converted waves. Stork (2020) shows that land seismic data suffer from microscattering in the small-scale heterogeneities of the near surface,

which at times can greatly reduce the signal transmitted to deeper events.

Recent successful applications of FWI in the Permian Basin (Bai et al., 2020; Murphy, 2020; Bai et al., 2021) have shown that it remains a challenge in land processing to take full advantage of the recorded energy below 5 Hz due to the highly variable signal-to-noise ratio (S/N), even with nonlinear sweeps starting as low as 2 Hz. These very low frequencies are challenging to generate with hydraulic vibroseis due to the necessary increase in time spent sweeping frequencies below 4 Hz to produce adequate S/N (Winter et al., 2014). To be more efficient, vibrators require larger-reaction mass strokes, which are restricted by actuator size and pump capacity. They are also constrained to a lesser extent by potential resonance within the truck’s support frame (see Meunier [2011] for a more extensive explanation of vibroseis limitations on low frequencies). Some design modifications to standard vibroseis have been proposed recently to overcome these limitations (Noorlandt, 2015; Wei, 2016). However, to our knowledge they have not been commercially deployed in the United States at this time. Even when very low frequencies are present on the energy emitted by the source, onshore near-surface complexity and non-negligible elastic phenomena in the ground usually make them very noisy. Geophone sensitivity below their natural frequency (e.g., 10 Hz) may also significantly impact their quality and phase stability, especially when S/N is low (Roux et al., 2014). On the other hand, the long offsets are also heavily impacted by low S/N and guided waves.

We can expect the Permian Basin to be particularly challenging in this respect, especially west of the Delaware Basin where the Cenozoic fill is present. Successful onshore broadband seismic case studies in other parts of the world have been published (Winter et al., 2014; Saleh et al., 2017). However, they were either located in different geologic settings or acquired in areas free of dense infrastructure and private land ownership, where much higher trace density helped maximize the benefits of broadband sweeps. Therefore, it is legitimate to question the extent of the usefulness of very low frequencies and far offsets for onshore seismic exploration in the Permian Basin to achieve the end purpose of earth model inversion and reservoir imaging, given the effort involved to record them (and the significant cost they add to surveys in this region). In this paper, we attempt to answer this question on a dense survey recently acquired in the Central Basin Platform of

<sup>1</sup>CGG, Houston, Texas, USA. E-mail: vincent.durussel@cgg.com; scott.downie@cgg.com.

<sup>2</sup>CGG, Calgary, Canada. E-mail: dongren.bai@cgg.com; amin.baharvand@cgg.com.

<sup>3</sup>Occidental Petroleum, Houston, Texas, USA. E-mail: keith\_millis@oxy.com.

the Texas oil province. We will first share details on the acquisition as well as the main features considered important for the acquisition design. We will then discuss several imaging aspects, such as FWI, final migrated seismic, and quantitative interpretation.

### Acquisition design and preplanning

The goals of this program were to image targets throughout the sedimentary section, provide the processing team with sufficient sampling to adequately attenuate surface waves, and capture the low frequencies and far offsets that are crucial for successful FWI. An evaluation of data from legacy programs and an analysis of the expected processing workflow highlighted the need for relatively tight line and station intervals, as well as a sizeable patch. A map of the 595 mi<sup>2</sup> survey is shown in Figure 1. As the program was to be acquired with nodal receivers, many additional offsets could be made available outside of the predefined acquisition patch.

Permitting began in May 2019 for a planned start of recording by December of the same year. This was a small window, considering the sizable area and the number of landowners in and around the city of West Odessa. Before the start of the main survey, several tests were conducted to assess optimum parameters, as is often the case for vibroseis acquisitions. These tests went further than typical single location sweep tests and incorporated two complete perpendicular 2D lines. While the primary aim of these tests was to establish a fit-for-purpose sweep to be used during the acquisition, a secondary aim was to determine the efficacy of

a single vibroseis per source location, as opposed to the conventional two vibrators. A description of the 2D test parameters is shown in Figure 2. While the results of the vibroseis per shot point comparison are outside the scope of this paper, acceptable results from one vibroseis per shot point were established. Nevertheless, due to the multiclient nature of this project and the need for a good S/N on far offsets, the decision was made to continue the project with two vibroseis per shot point.

Figure 3 shows a field shot acquired with two different sweeps: 3–96 Hz EmphaSeis (Figures 3a and 3b) and low-dwell 1.5–110 Hz (Figures 3c and 3d). Figures 3a and 3c show the full bandwidth, and Figures 3b and 3d show data with a 5–8 Hz high-cut filter applied to isolate low frequencies. A geophone response filter was also applied to the data. Continuous reflections are sometimes difficult to track on field shots in the Permian Basin, but here some can be clearly observed at full bandwidth almost all the way to the farthest offsets (left-hand side of the shot; approximately 23,000 ft). However, they are very hard to see at the low end of the spectrum (Figures 3b and 3d), making it difficult to make an informed decision as to which sweep to use solely on the basis of these data. As a backup, the strength and continuity of diving and guided waves observed on such sweep tests often guide the selection of the starting frequency in the Permian Basin. However, as can be seen in Figures 3b and 3d, the benefits on low frequencies brought by the 1.5–110 Hz low dwell are inconclusive.

### Main 3D acquisition

The main 3D survey was then acquired, and the recording crew arrived on site as scheduled on 20 December 2019 with the first vibrator point recorded on 30 December. The crew faced many challenges in the area, with the heavily urbanized areas of West Odessa combined with a large amount of oil-field infrastructures. Low power lines, flow lines, and oil-field traffic were daily concerns. The recording crew performed very well to overcome these challenges in the midst of a global pandemic. The program was completed safely without incident on 17 July 2020 and averaged more than 2400 vibrator points per day. Resolution was a key factor for all stakeholders, and small station intervals (82.5 ft) and line spacing (495 ft) was chosen for sources and receivers. Note that illustrating the merits of high trace density for time-lag FWI (TLFWI) is beyond the scope of this paper. See Bai et al. (2021)



Figure 1. Outline and location of the 2020 Central Basin Platform (CBP1) seismic survey.

2D Test line Sweeps													
Test #	Freq Low	Freq High	Freq Range (octaves)	Sweep Length	Number of Vibes Per Fleet	RP Interval (ft)	SP Interval (ft)	Bin size for line	Line processed	Number of VPs	Number of vibe fleets	Harmonic Noise present	Slip Time between VPs (sec)
A1*	3	96	5.0	24	2	82.5	82.5	41.25	NS	384	2	Small	16
A2	3	96	5.0	24	2	41.25	82.5	20.625	NS	384	2	Small	16
B1	3	96	5.0	24	2	82.5	41.25	20.625	NS	768	2	Small	16
B2*	3	96	5.0	24	2	41.25	41.25	20.625	NS	768	2	Small	16
C	3	96	5.0	24	1	41.25	41.25		NS	768	4	yes	5
D1*	1.5	110	6.2	24	1	82.5	82.5	41.25	NS & WE	1280	4	yes	5
D2	1.5	110	6.2	24	1	82.5	41.25	20.625	NS & WE	1280	4	yes	5
D3	1.5	110	6.2	24	1	41.25	41.25	20.625	NS & WE	1280	4	yes	5
E1	4	110	4.8	12	1	41.25	41.25		NS	768	4	deblend	0
E2	4	110	4.8	12	1	41.25	41.25		NS	768	4	deblend	0
E3	4	110	4.8	12	1	41.25	41.25		NS	768	4	deblend	0
F	4	110	4.8	12	1	41.25	41.25		NS	100	4	No	17

Figure 2. Summary of the parameters tested on the short 2D program acquired prior to the main 3D survey. The aim was to refine the design for optimum very low frequencies, long offsets, and trace density.

for a discussion on this topic. The wavefield was generated with two vibroseis per source point and recorded with three-element receiver arrays. The recording geometry was 64 × 384 nodes, providing sufficiently long offsets for FWI (maximum offset of approximately 23,000 ft to deliver a maximum diving-wave penetration of approximately 5000 ft). It resulted in a rather dense survey, with 1024 nominal fold at 41.25 × 41.25 ft bin size. The 1.5 Hz starting frequency would either add significant length to the sweep or decrease signal strength for the mid and high end of the

spectrum. However, bearing in mind the need for good low-frequency content for FWI, a 2 Hz starting frequency was retained as a reasonable compromise. As a result, the selected sweep (also guided by tests described in the previous section and by stakeholder experience in the area) was 2–96 Hz low dwell with custom tapers (24 s length).

An example field shot with increasing high-cut frequencies to better isolate the low end of the bandwidth is shown in Figure 4. Only surface wave attenuation and geophone compensation (to gain and rephase low frequencies) were applied to these data without low-cut filtering of any type. If continuous diving waves can be observed on the 5 and 6 Hz panels, their energy is only marginally observable on 4 Hz. As for 3 Hz and below, they are either absent or so weak that the naked eye cannot track them. Figure 4 illustrates the difficulty in assessing the presence and quality of very low-frequency energy on single-fold data in the Permian Basin. However, the 5 and 6 Hz diving-wave energy can be tracked almost all the way to far offsets (approximately 20,000 ft on this display), whereas the amplitude of higher frequencies (30 Hz panel) quickly becomes attenuated beyond approximately 15,000 ft.

However, the raw unmigrated stack shown in Figure 5 exhibits some coherent reflections at least as low as 3 Hz (Figure 5b), although it is still heavily affected by noise and uncollapsed diffractions at this stage. The processing applied for this stack was very basic and only involved geophone correction, spherical divergence, preliminary statics, normal moveout corrections, and prestack amplitude gain correction. One can speculate that the main factor in making these reflections more coherent on the brute stack than diving waves are on field shots (Figure 4) is probably the stacking process, which is well known to have a powerful denoising effect. Hence, despite no convincing evidence from raw shots, we can conclude from brute stacking that these very low frequencies (2–5 Hz) were indeed emitted by the source and recorded by the node arrays with enough S/N to make them trackable on an unmigrated stack.

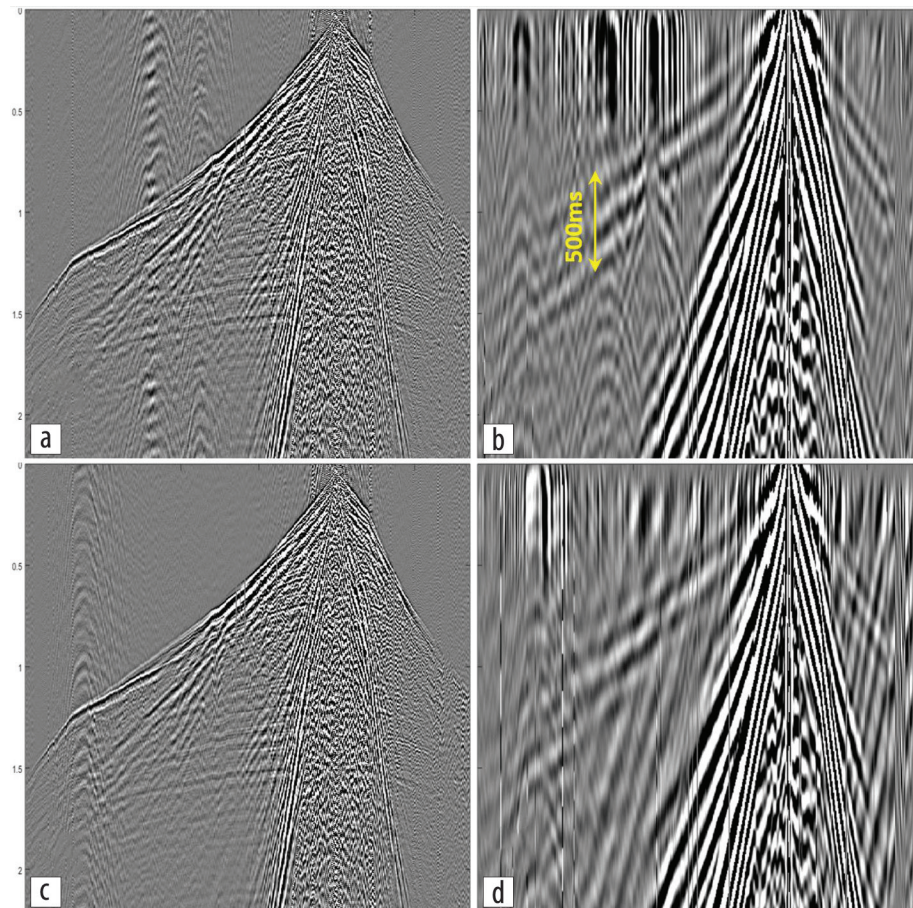


**Figure 3.** Sweep test performed before the beginning of the main program. (a) The 3–96 Hz EmphaSeis sweep at full bandwidth. (b) The 3–96 Hz EmphaSeis sweep with 5–8 Hz high-cut filter. (c) The 1.5–110 Hz low-dwell sweep at full bandwidth. (d) The 1.5–110 Hz low-dwell sweep with 5–8 Hz high-cut filter. Vertical axis is in time (s). Geophone compensation was applied to the data.

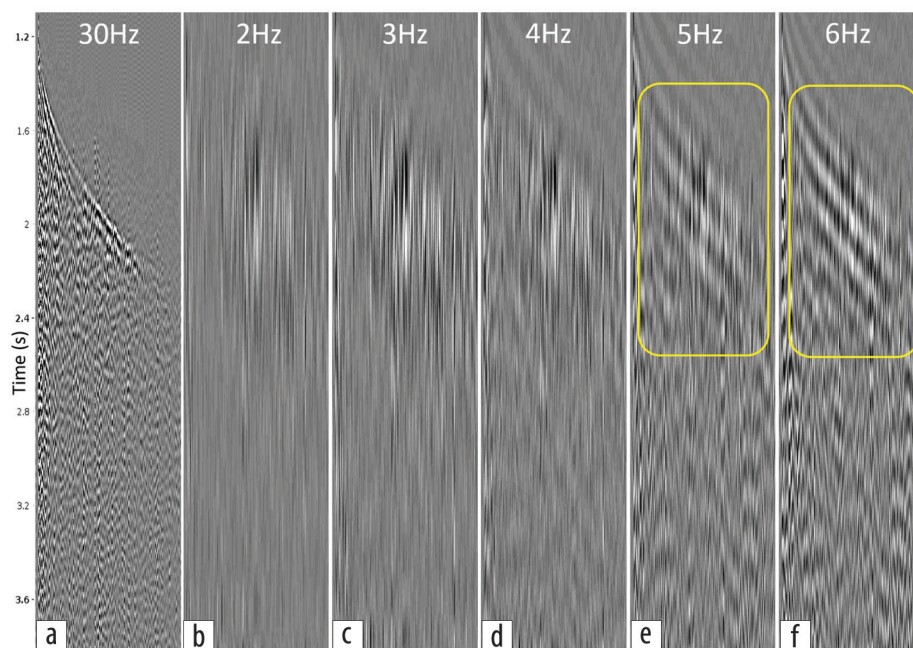


**Figure 4.** Field shot after surface wave attenuation and geophone compensation from the 3D main survey (2–96 Hz low-dwell sweep) with (a) 30 Hz, (b) 2 Hz, (c) 3 Hz, (d) 4 Hz, (e) 5 Hz, and (f) 6 Hz Chebychev high-cut filter. Barely any coherent diving- and guided-wave energy can be detected by eye below 5 Hz. The maximum offset shown here is 20,000 ft.

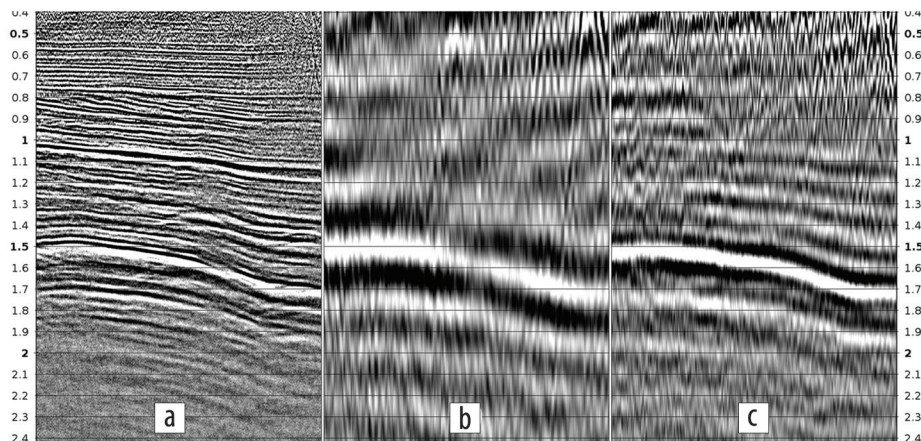


**Figure 5.** Brute stack from the 3D main survey 2–96 Hz low-dwell sweep at (a) full bandwidth, (b) 2–4 Hz octave, and (c) 4–8 Hz octave. Vertical axis is two-way time (s).

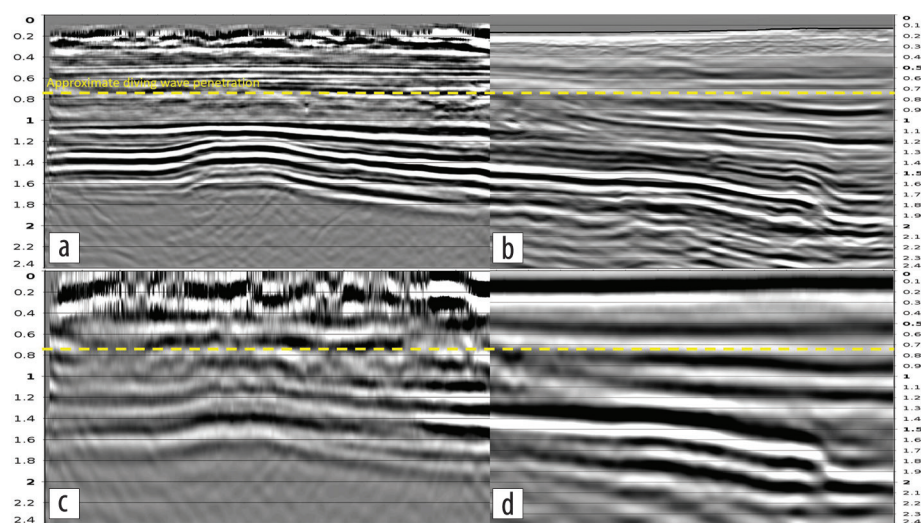


**Figure 6.** Comparison between (b) 20 Hz TLFWI image (stretched to time) and (a) final PSTM stack with low-pass filter applied to match the TLFWI bandwidth. (c) and (d) The 2–4 Hz octave for each corresponding top section. The vertical axis is time (s). The yellow dotted line shows the approximate diving-wave penetration (approximately 5000 ft) from the approximately 23,000 ft maximum offset recorded. As a comparison, reducing the maximum offset to approximately 15,000 ft would have reduced diving-wave penetration by approximately 800 ft.

### FWI imaging and quantitative interpretation

TLFWI (Zhang et al., 2018) was applied to the entire data set to resolve the complex geology, including shallow evaporite, small anomalies, and extensive deep fault structures (Bai et al., 2021). The inversion was run up to 20 Hz, using both diving waves and reflections to allow deeper updates beyond diving-wave penetration. Bai et al. (2021) show that the presence of diving wave helps to reduce the sensitivity of TLFWI to the quality of the starting model. As a reference, reducing the maximum offset to 15,000 ft on the patch would have reduced the diving-wave penetration by approximately 800 ft. Despite the 2 Hz low-dwell sweep, diving-wave energy appears to have low S/N at very low frequency as shown in Figure 4. Therefore, a starting frequency of 5 Hz was used for FWI but also included a very low-frequency component down to 3 Hz. The initial model was built from refraction tomography and well sonic logs followed by reflection tomography and well calibrations to provide a starting model with

good low wavenumber background velocity and to minimize the risk of cycle skipping or convergence toward local minima. An FWI image was output from 20 Hz TLFWI inversion as an additional product (Huang et al., 2021). Figures 6a and 6b show a certain comparison of the TLFWI image (stretched to the time domain) and final prestack time migration (PSTM) seismic with a low-pass filter applied to match the 20 Hz TLFWI bandwidth. The combination of kinematic tomography and FWI was able to retrieve a crisp reflectivity all the way up to the surface, mostly relying on refracted energy above approximately 500 ms. Recorded reflections do not generally have sufficient coverage to generate a clear seismic image of the near surface. Figures 6c and 6d show the 2–4 Hz octave for the two corresponding sections above. The TLFWI was still able to estimate continuous velocity perturbations, which are conformable with geology in that very low frequency band, even beyond diving-wave penetration, despite lower S/N on recorded seismic.

To complete the assessment of amplitude fidelity in the very low-frequency band, an acoustic inversion was run on the final PSTM migration. Extra attention was paid to the phase processing using available well information. A geophone filter, surface-consistent deconvolution, phase-only  $Q$  compensation, and extra phase rotation of  $60^\circ$  were applied to the final seismic to match zero-phase well synthetics.

Six wells were used to build the low-frequency model using logs up to 2 Hz (full taper on at 3 Hz) to highlight seismic amplitude fidelity at the start of the bandwidth. An additional well was kept blind (to build the initial model and for parameterization of the model-based inversion) with results shown in Figure 7. Figure 7a shows the full-bandwidth impedance, Figure 7b shows its low-frequency component (5–7 Hz high cut), and Figure 7c shows a low-frequency model built from guiding horizons using well logs up to 7 Hz. The latter would essentially be the inverted impedance in that bandwidth if no energy was recorded on seismic at 7 Hz and below. Although S/N is still lower than for the mid-frequency range, the match with the blind log at target level (soft blue layer) is quite reasonable (Figure 7b). The very low-frequency part of the seismic bandwidth and long offsets are key to invert the compressional fault system on the left of the section (circled area). These sharp geologic variations would not be present on an inversion relying

solely on sparse well data for the low end of the bandwidth (Figure 7c).

## Conclusions

Estimating cost versus benefits is always a difficult exercise, especially when a complex workflow is involved, and many external factors impact the final result. Although the latest advances in acquisition and processing enable onshore seismic to catch up with offshore to some extent, S/N remains poorer overall on onshore seismic (due to near-surface scattering, elastic effects, vibroseis limitations, etc.). As a result, as illustrated in this paper, it is still very challenging to evaluate the very low-frequency part of the bandwidth and the signal present on far offsets on raw seismic records in the Permian Basin, even with two vibroseis per shot point and low-dwell sweeps. Increasing source strength by using more vibroseis per shot point or better noise filtering with larger geophone arrays could help with both aspects. However, this would also significantly increase the cost and remove the benefits associated with point-source acquisitions.

Near-surface conditions can also greatly bias the choice of sweep parameters driving the bandwidth, and decisions are sometimes made on energy observed on raw records that will not eventually contribute to the final image. Despite all of these complications, we demonstrated in this study that the very low-frequency component enriched by low-dwell profiles can still be recorded reliably and bring valuable information to finished seismic products for reservoir imaging in West Texas. The longer far offsets recorded on this new survey also helped stabilize the TLFWI results in the overburden and retrieve small-scale shallow velocity heterogeneities. Nevertheless, because S/N is lower on very low frequencies and long offsets, it requires extra care and effort when recorded and processed (e.g., high-end noise attenuation techniques, rephrasing, and signal preservation). Although partially limited by modeling resolution, the FWI image (Figure 6) exhibits very good inverted signal continuity on very low frequencies. Whereas, the migrated seismic may still have some remnant noise, but hopefully preserves recorded amplitudes in their full integrity. The two complement each other somewhat in this study, which shows that TLFWI is an important tool for maximizing quality of information retrieved in the near surface, where earth properties cannot be inverted using kinematic reflections alone. Very low frequencies and longer offsets bring value in this respect and help bridge the gap with other ground measurements, even in challenging conditions. ■■

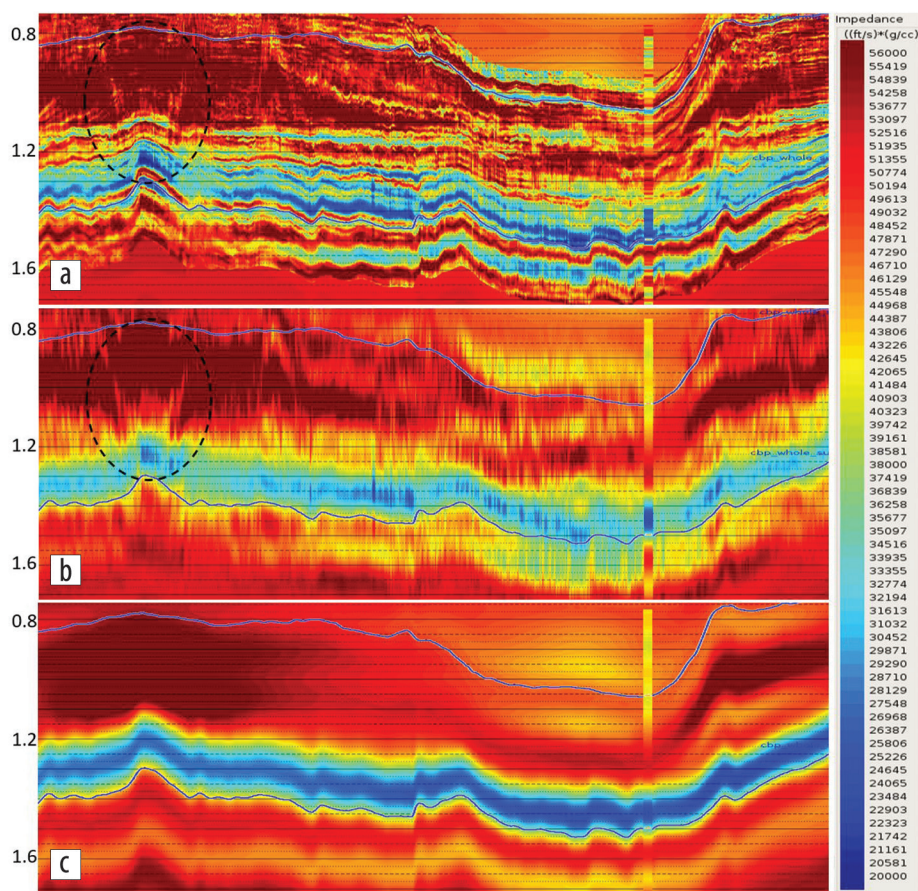


**Figure 7.** Acoustic impedance inversion on final PSTM. (a) The full-bandwidth inverted impedance. The well shown is a blind well (not used for the inversion). (b) Inverted very low-frequency component only (5–7 Hz high cut). (c) A low-frequency model created from wells only (with a 5–7 Hz high-cut filter). Vertical axis is two-way time (s). The circled area shows a compression fault system, which would not be properly inverted if relying solely on low frequencies from sparse well data.

## Acknowledgments

The authors thank CGG Multi-Client and OXY for permission to publish this work. We would also like to recognize the significant contributions made by CGG colleague Anna Leslie, particularly to the survey design. We thank Dawson for the outstanding quality of their acquisition work as well as CGG's Calgary Subsurface Imaging Team for their processing excellence. The authors also thank CGG colleagues who reviewed the draft (especially Shuo Ji, Joe Zhou, and Lin Zheng).

## Data and materials availability

Data associated with this research are confidential and cannot be released.

Corresponding author: vincent.durussel@cgg.com

## References

- Bai, D., F. Hou, and J. Hefti, 2020, A case study in the Delaware Basin: Application of time-lag FWI and 3D SRME/IMA multiple attenuation: Presented at Geoconvention.
- Bai, D., L. Zheng, and W. Deng, 2021, Imaging the complex geology in the Central Basin Platform with land FWI: First International Meeting for Applied Geoscience & Energy, SEG/AAPG, Expanded Abstracts, <https://doi.org/10.1190/segam2021-3583769.1>.

- Duval, G., 2012, How broadband can unlock the remaining hydrocarbon potential of the North Sea: *First Break*, **30**, no. 12, <https://doi.org/10.3997/1365-2397.30.12.65621>.
- Huang, R., Z. Zhang, Z. Wu, Z. Wei, J. Mei, and P. Wang, 2021, Full-waveform inversion for full-wavefield imaging: Decades in the making: *The Leading Edge*, **40**, no. 5, 324–334, <https://doi.org/10.1190/tle40050324.1>.
- Le Meur, D., D. Donno, J. Courbin, D. Solyga, and A. Prescott, 2020, Retrieving ultra-low frequency surface waves from land blended continuous recording data: 90<sup>th</sup> Annual International Meeting, SEG, Expanded Abstracts, <https://doi.org/10.1190/segam2020-3418624.1>.
- Meunier, J., 2011, Seismic acquisition from yesterday to tomorrow: SEG.
- Murphy, G., V. Brown, and D. Vigh, 2020, Land FWI in the Delaware Basin, West Texas: A case study: *The Leading Edge*, **39**, no. 5, 324–331, <https://doi.org/10.1190/tle39050324.1>.
- Noorlandt, R., G. Drijkoningen, J. Dams, and R. Jenneskens, 2015, A seismic vertical vibrator driven by linear synchronous motors: *Geophysics*, **80**, no. 2, EN57–EN67, <https://doi.org/10.1190/geo2014-0295.1>.
- Reiser, C., and T. Bird, 2016, Advances in broadband quantitative interpretation: 86<sup>th</sup> Annual International Meeting, SEG, Expanded Abstracts, <https://doi.org/10.1190/segam2016-13818140.1>.
- Roux, P.-F., B. de Cacqueray, and C. Maisons, 2014, Conventional sensors: Is there anything useable below their natural frequency?: 84<sup>th</sup> Annual International Meeting, SEG, Expanded Abstracts, <https://doi.org/10.1190/segam2014-1506.1>.
- Sablon, R., Y. Lafet, D. Lin, and R. Soubaras, 2012, Challenges and benefits of variable-depth streamer: From acquisition to interpretation: 82<sup>nd</sup> Annual International Meeting, SEG, Expanded Abstracts, <https://doi.org/10.1190/IST092012-001.18>.
- Saleh, A., A. El. Fiki, J. M. Rodriguez, S. Laroche, K. Y. Castor, D. Marin, T. Bianchi, P. Bertrand, and P. Herrmann, 2017, A step change in seismic imaging quality in Western Desert of Egypt — An acquisition case study: Presented at the 79<sup>th</sup> Conference and Exhibition, EAGE.
- Stork, C., 2020, How does the thin near surface of the earth produce 10–100 times more noise on land seismic data than on marine data?: *First Break*, **38**, no. 8, 67–75, <https://doi.org/10.3997/1365-2397.fb2020062>.
- ten Kroode, F., S. Bergler, C. Corsten, J. W. de Maag, F. Strijbos, and H. Tijhof, 2013, Broadband seismic data — The importance of low frequencies: *Geophysics*, **78**, no. 2, WA3–WA14, <https://doi.org/10.1190/geo2012-0294.1>.
- Wei, Z., 2016, A new low-frequency vibrator enhances blended vibroseis acquisition: 86<sup>th</sup> Annual International Meeting, SEG, Expanded Abstracts, <https://doi.org/10.1190/segam2016-13174103.1>.
- Winter, O., A. Leslie, F. Lin, and P. Maxwell, 2014, Acquiring low frequencies onshore: Sweep, sensors, sampling and stories: *CSEG Recorder*, **39**, no. 6.
- Yao, Y., H. Ma, Y. Liu, C. Peng, G. Mohapatra, G. Duncan, W. Martins, and S. Checkles, 2019, Improving images under complex salt with ocean bottom node data: 89<sup>th</sup> Annual International Meeting, SEG, Expanded Abstracts, <https://doi.org/10.1190/segam2019-3216820.1>.
- Zhang, Z., J. Mei, F. Lin, R. Huang, and P. Wang, 2018, Correcting for salt misinterpretation with full-waveform inversion: 88<sup>th</sup> Annual International Meeting, SEG, Expanded Abstracts, <https://doi.org/10.1190/segam2018-2997711.1>.